



Research article

A mathematical model for Zika virus disease: Intervention methods and control of affected pregnancies

Chad Westphal^{1,*}, Shelby Stanhope², William Cooper^{3,4} and Cihang Wang¹

¹ Department of Mathematics and Computer Science, Wabash College, Crawfordsville, IN, USA

² Department of Mathematical Sciences, U.S. Air Force Academy, USAF Academy, CO, USA

³ College of Medicine, Texas A&M University, Temple, TX, USA

⁴ United States Air Force, USA

* **Correspondence:** Email: westphac@wabash.edu; Tel: +17653616101.

Abstract: Zika virus is spread to human populations primarily by *Aedes aegypti* mosquitoes, and Zika virus disease has been linked to a number of developmental abnormalities and miscarriages, generally coinciding with infection during early pregnancy. In this paper, we propose a new mathematical model for the transmission of Zika and study a range of control strategies to reduce the incidence of affected pregnancies in an outbreak. While most infectious disease models primarily focus on measures of the spread of the disease, our model is formulated to estimate the number of affected pregnancies throughout the simulated outbreak. Thus the effectiveness of control measures and parameter sensitivity analysis is done with respect to this metric. In addition to traditional intervention strategies, we consider the introduction of Wolbachia-infected mosquitoes into the native population. Our results suggest a threshold parameter for Wolbachia as an effective control measure, and show the natural time scale needed for Wolbachia-infected mosquitoes to effectively replace the native population. Additionally, we consider the possibility of a Zika vaccine, both to avoid an outbreak through herd immunity and as a control measure administered during an active outbreak. With emerging data on persistence of Zika virus in semen, the proposed compartmental model also includes a component of post-infectious males, which introduces a longer time scale for sexual transmission than the primary route. While the overall role of sexual transmission of Zika in an outbreak scenario is small compared with the dominant human-vector route, this model predicts conditions under which subpopulations may make this secondary route more significant.

Keywords: Zika; infectious disease model; parameter sensitivity; microcephaly; congenital Zika syndrome; Wolbachia

1. Introduction and background

While the Zika virus has been known since the 1940s, only recently has Zika virus disease gone from being a *neglected tropical disease* to being a significant concern on a global scale. Following a particularly large outbreak in Brazil and Colombia in 2015 and 2016 [1,2], studies have shown a widespread distribution throughout the Americas [3]. Transmitted primarily by the *Aedes aegypti* mosquito, Zika is a vector-borne disease that spreads most easily in places with high rates of human/mosquito contact. While not particularly dangerous for most healthy adults who contract the disease, Zika has been linked to an increased incidence of developmental abnormalities for infants born to mothers infected during early pregnancy. For example, in the aftermath of the Brazil outbreak nearly 2000 cases of microcephaly (a rare condition related to abnormal *in utero* brain development) were confirmed to be related to the infection [4,5]. Outcomes in Colombia have shown that women with confirmed infections during the first trimester experienced elevated rates of pregnancy loss and live births with higher incidence of low birth weight, preterm delivery, and brain or eye defects [2,6]. While it is clear that Zika virus disease is a threat to developing fetuses, there is still much that is unknown [7]. With this understanding, controlling the spread of Zika has become an issue of worldwide significance.

Following the 2015–2016 outbreaks in Brazil and Colombia, the effective use of mathematical models for Zika dynamics has played an important role in understanding the disease and its effects. Understanding the dynamics of the spread of infectious diseases is an important tool to aid in assessing the likely effectiveness of control measures [8–10]. Given that the primary concern of Zika is the potential for developmental interruptions, analytic models and intervention strategies for Zika are necessarily different from those for other more well-known arboviruses.

Mathematical models for Zika dynamics in the current literature indicate that the human-vector interaction and vector death rates are most significantly correlated with the spread of Zika [11–13]. The role of sexual transmission of Zika remains an area of active research [14–21], where studies indicate that sexual transmission is likely a significant secondary contributor to the spread of the disease and on a potentially different time scale as the primary human-vector route. Importantly, the virus remains detectable in human semen for months in the post-infection period [22,23]. Another potentially important transmission route is the possibility of vertical transmission from adult female mosquitoes to eggs [24].

Other models in the literature have studied various aspects related to the spread of Zika virus disease. For example, in [25] seasonal conditions that led to time-dependent mosquito birth/death rates were considered in a model of Zika spread. These considerations may be important since the time scale of an outbreak is likely to span the wet/dry seasons. A network model was developed in [26], and [27] reviewed a range of other recent work related the spatial dependence of Zika dynamics. Since the geographic range of a Zika outbreak may be quite large, the ways that spatial differences contribute to the understanding of Zika dynamics may also be important.

In addition to the typical range of possible control measures for Zika, modifying the native mosquito population is a possibility of emerging interest. In [28], a sterile insect technique was investigated. Similarly, the World Mosquito Program (<https://www.worldmosquitoprogram.org/>) developed a technique to introduce *Aedes aegypti* mosquitoes infected with Wolbachia, which is a bacteria that reduces the ability of the Zika virus to reproduce in the gut of infected mosquitoes. Recent studies have shown this to be effective in providing a level of protection against dengue, yellow fever, and chikungunya [29–31].

Mathematical models of Zika virus have included Wolbachia mosquito dynamics. For example, [32] investigated how releasing male vs female Wolbachia infected mosquitoes impacts the spread of Zika virus, and [33] incorporated the release of Wolbachia infected males mosquitoes in a stochastic model of Zika virus transmission. A range of ordinary differential equation (ODE) models for Wolbachia spread were presented in [34], which showed that even simplified reduced order models can effectively capture the most important aspects of the dynamics.

Currently there is no Zika vaccine available, though there are candidates under study [35,36]. Moreover, while the availability of an effective vaccine would be a promising step in preventing future outbreaks, it is still important to understand how to combat an outbreak as it occurs in a population that isn't sufficiently protected. The impact of a Zika virus vaccination on the basic reproduction number \mathcal{R}_0 was modeled in [37], with various levels of vaccine efficacy considered. Additionally, in [38] vaccination was treated as a control in a spatial SIR model of Zika virus.

In this paper, we build on a vast and growing body of literature aimed at understanding the factors that are important in the spread of Zika and characterizing the ways that intervention methods can reduce the incidence of pregnancies with Zika-related complications. In particular, this study proposes a model for Zika transmission that includes a mechanism to estimate the number of affected pregnancies in a simulated outbreak. In evaluating control strategies, we use this metric as an indicator, rather than a general measure of transmissibility such as the basic reproduction number. We examine the effectiveness of traditional intervention strategies as well as the possibility of either a vaccine or the introduction of Wolbachia as a control measure in the *Aedes aegypti* mosquito population. In addition, our model includes a population of post-infectious male humans who may continue to infect their sexual partners due to the presence of Zika virus in their semen. This allows for a consideration of the role of sexual transmission in the spread and persistence of Zika virus in a population.

The organization of this paper is as follows: in Section 2, we introduce the proposed model for Zika transmission and give details on parameter selection and model calibration; the basic reproduction number and the herd immunity threshold is presented in Section 3; Section 4 focuses on the introduction of Wolbachia infected mosquitoes; Section 5 describes several other intervention strategies, and a sensitivity analysis of the associated control variables is given in Section 6; Section 7 explores the dynamics of sexual transmission of Zika, independent of the human-vector route; and finally, Section 8 provides a summary and discussion of the main results in this work.

2. Baseline mathematical model

In this section, we provide a description of the modeling assumptions and basic details of the proposed mathematical model for Zika dynamics given in Eq (2.1) and illustrated by the compartment model in Figure 1. Table 1 defines all of the state variables in the model, and Table 2 gives a description of each of the parameters, which are chosen to illustrate a baseline case that results in an outbreak.

The system consists of cohabiting populations of n_h people and n_v *Aedes aegypti* mosquitoes (i.e., vectors). Initially, most individuals are infection-free and susceptible (S and S_v for humans and mosquitoes, respectively), but there is a small number of either infected mosquitoes (I_v) or infected humans in the population. Infected humans will be either symptomatic (I_s) or asymptomatic (I_a). People infected typically recover (R) within a few weeks and are then considered immune from reinfection.

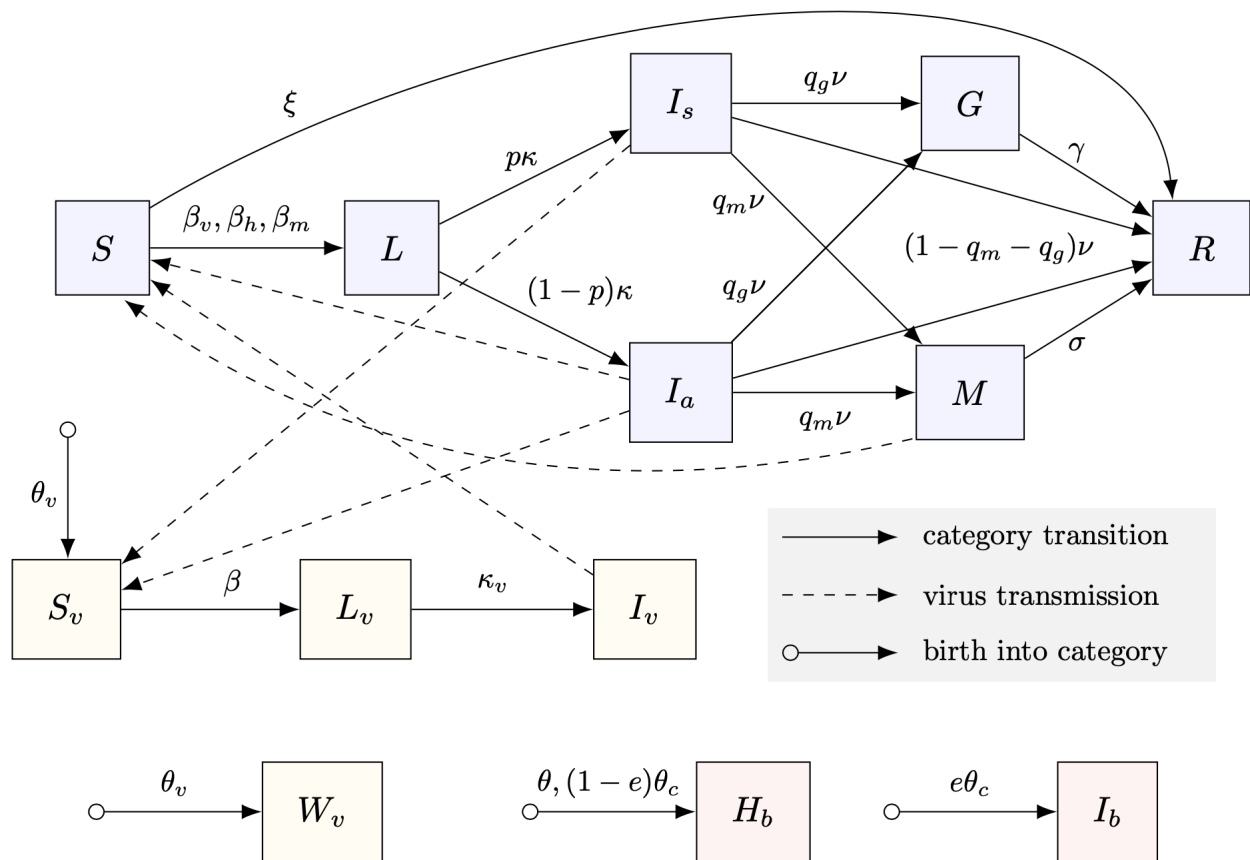


Figure 1. Proposed compartmental model for the dynamics of Zika. Additionally, each compartment has a natural death rate (not shown) with rate μ_v for each compartment of the vector population, $\mu + \alpha$ for symptomatic infected humans, and μ for all other humans. Descriptions of populations and parameters are given in Table 2.

We assume an average duration of infection of 10 days for both I_s and I_a populations [23]. Infected mosquitoes I_v remain infectious until death.

As the populations interact over time, the virus may be transmitted from an infected mosquito to a susceptible person (I_v to S) or from an infected person to a susceptible mosquito (I_s or I_a to S_v). The interaction parameters β_v and β represent the frequency of mosquito bites (as received per human and given per mosquito, respectively) conditioned on the probability of the bite transmitting the infection. These rates will obviously broadly vary across different scenarios. We describe how we choose the interaction parameters for our baseline scenario in Section 3.

Newly exposed humans or mosquitoes go through a latent phase (L and L_v , respectively), where the virus replicates in their system to the level where it can be transmitted. We assume the latent phase lasts an average of 7 days for humans [9, 39] and 10 days for mosquitoes [9, 12].

Zika virus may also be transmitted between humans through sexual contact between people from S and I_a , primarily through semen transfer. Additionally, we assume that the virus may remain viable in the semen of infected males for an average of 54 days after the virus has been cleared from their

Table 1. Description of the state variables in Figure 1 and Eq (2.1), with units being the number of individuals in each group.

State variables	Definition
S	susceptible, infection-free humans
L	latent humans (recently exposed, but cannot yet transmit virus)
I_a	infected, asymptomatic humans
I_s	infected, symptomatic humans
G	post-infectious women of childbearing age
M	male sub-population who are able to transmit Zika virus sexually
R	recovered humans
S_v	susceptible, infection-free mosquitoes
L_v	latent mosquitoes (recently exposed, but cannot yet transmit virus)
I_v	infected mosquitoes
W_v	Wolbachia mosquitoes
H_b	births unaffected by Zika virus infection
I_b	births affected by Zika virus infection

bloodstream (see [22, 23]). Thus, upon recovery we hold the proportion of potentially sexually active males to the general population in M before they are considered in R . We consider sexual transmission between people from M and S , which occurs at twice the rate as between I_a and S (since M is necessarily populated by males).

Infected humans will be either symptomatic (I_s , with probability p) or asymptomatic (I_a , with probability $1 - p$). People in I_s typically develop flu-like symptoms, similar to many other tropical diseases. We assume a value of $p = 0.2$, which is based on clinical data following the 2007 Yap Islands outbreak [40] and has been widely used in modeling studies (e.g., [9, 12]). A more recent 2018 meta-analysis study in [41] found consistent results, but noted that a significant amount of uncertainty remained in this statistic. The presence of symptoms is important to consider, as it will impact the behavior of the individual, and thus the transmission of the disease. We assume that individuals who have symptomatic Zika infection (individuals in I_s) will not interact with individuals in S because the symptoms of Zika will cause them to refrain from sexual activity while they are ill. Thus, the model does not include a transmission pathway between I_s and S .

The context of the interactions between mosquitoes and humans greatly varies depending on living conditions. For example, there are contexts in which one might assume that the majority of interactions between humans and mosquitoes only occur outside the home; but in other circumstances, interactions between humans and mosquitoes are most likely to occur overnight, while the individual is sleeping (e.g., in open housing without a net). Thus, we assume that the interactions between infected humans and mosquitoes does not depend on whether or not the human is symptomatic, as we cannot infer whether resting at home will increase or decrease the interactions with mosquitoes.

If an infection occurs in early pregnancy, then there is a possibility that the virus will cause de-

developmental abnormalities, and we consider the case as an affected pregnancy. This includes births potentially categorized as *Congenital Zika Syndrome* or in a pregnancy that is not viable [5]. We define G as the subset of recovered women who could possibly have been pregnant while infected (i.e., post-infectious women of childbearing age). Since individuals in G could have experienced infection anytime during pregnancy, we choose the rate from G to R so that the expected value of time in G is 4.5 months.

The birth rate relative to G is necessarily higher than relative to the entire population, and births will be considered unaffected/healthy, H_b , or affected by the infection, I_b . We take the effective probability of infection affecting a pregnancy as $1/3$, which is consistent with the mother's infection occurring during the first trimester. The final asymptotic value of I_b represents an estimate of the number of pregnancies that could experience any of the negative outcomes known to be associated with Zika that would otherwise have been a normal/unaffected birth. Populations S , L , I_s , I_a , and R produce healthy births at a rate consistent with an average birth rate relative to the total population. All human populations except for H_b and I_b have a natural death rate, typically chosen to match the natural birth rate of the population. Symptomatic infected humans, I_s , have an elevated death rate due to secondary complications. We assume that this rate is of a magnitude similar to the overall background population, reflecting the consensus that Zika is only a marginal threat to the general population.

We assume population statistics relative to Colombia as reported in the 2018 census [42]. Thus we assume the fraction of women of childbearing age (15–44 years) to total population of 23.7%, the fraction of men of sexually active age (15–64 years) to the total population of 31.3%. The average birth rate relative to the total population is taken as $0.0000433 \text{ day}^{-1}$, and the birth rate relative to women of childbearing age is $0.000183 \text{ day}^{-1}$.

The model assumes that mosquitoes do not pass the virus to their offspring, though vertical transmission is increasingly considered possible [24]. This could be a contributor to a long term persistence of Zika in a region, but would likely be small relative to the predominant transmission routes in an active outbreak such as we consider in this paper. The mosquito birth/death rates significantly vary with temperature and precipitation [43]. We assume rates that correspond to an adult life span of 20 *days*, which corresponds to environmental conditions that are favorable to an outbreak (see [44] for details).

We consider the possibility of introducing Wolbachia-infected mosquitoes to the population, W_v , which are well-mixed into the mosquito population. The benefit is that Zika virus cannot develop to infectious levels within Wolbachia-infected mosquitoes, making W_v mosquitoes effectively immune from becoming carriers of Zika.

Mosquito eggs from females in W_v will result in Wolbachia-infected offspring (the male parent can be either W_v or non- W_v). Mosquito eggs from non- W_v females with males from W_v will not be viable. Only mosquito eggs resulting from parents who are both non- W_v will be non- W_v . This results in an emergence bias where Wolbachia becomes endemic through replacement over several generations. For example, in the case where half of the mosquito population is W_v , then the net birth rate into W_v will be twice that of into S_v . This observation is used to model the bias between the emergence into the W_v and S_v populations, as seen in system (2.1).

We consider the initial mosquito population fully saturated for the environment, where choosing the net birth rate equal to the net death rate leads to a constant total number of mosquitoes. Reducing the net birth rate or increasing the net death rate will result in a reduction in the population over time. Furthermore, we assume that the death rate for Wolbachia-infected and non-infected mosquitoes

are equal.

While our approach includes a relatively simplified model of Wolbachia infection, we note that further segmenting the mosquito population by sex, gestational status, and age is possible, and that studies such as those in [29, 30, 34, 45] considered a much wider range of the factors associated with Wolbachia dynamics.

In this study, we focus on the expected value of the number of affected births as a result of a Zika epidemic, and how this value can be reduced by specific intervention methods.

The ODE system for the proposed model is given by the following:

$$\begin{aligned}
 \frac{dS}{dt} &= -\left(\frac{\beta_v I_v}{n_v} + \frac{\beta_h I_a + \beta_m M}{n_h} + \mu + \xi\right)S \\
 \frac{dL}{dt} &= \left(\frac{\beta_v I_v}{n_v} + \frac{\beta_h I_a + \beta_m M}{n_h}\right)S - (\kappa + \mu)L \\
 \frac{dI_s}{dt} &= \kappa p L - (\nu + \mu + \alpha)I_s \\
 \frac{dI_a}{dt} &= (1 - p)\kappa L - (\nu + \mu)I_a \\
 \frac{dG}{dt} &= q_g \nu (I_s + I_a) - (\gamma + \mu)G \\
 \frac{dM}{dt} &= q_m \nu (I_s + I_a) - (\sigma + \mu)M \\
 \frac{dR}{dt} &= (1 - q_g - q_m)\nu (I_s + I_a) + \gamma G + \sigma M + \xi S - \mu R \\
 \frac{dS_v}{dt} &= \theta_v \left(1 - \frac{2W_v}{3n_v}\right)(S_v + L_v + I_v) - \left(\frac{\beta(I_s + I_a)}{n_h} + \mu_v\right)S_v \\
 \frac{dL_v}{dt} &= \frac{\beta(I_s + I_a)S_v}{n_h} - (\kappa_v + \mu_v)L_v \\
 \frac{dI_v}{dt} &= \kappa_v L_v - \mu_v I_v \\
 \frac{dW_v}{dt} &= \theta_v \left(1 + \frac{2}{3} \left(\frac{S_v + L_v + I_v}{n_v}\right)\right)W_v - \mu_v W_v \\
 \frac{dH_b}{dt} &= \theta(S + L + I_s + I_a + R) + (1 - e)\theta_c G \\
 \frac{dI_b}{dt} &= e\theta_c G,
 \end{aligned} \tag{2.1}$$

which includes net interacting human and vector population values given by $n_h = S + L + I_s + I_a + G + M + R$ and $n_v = S_v + L_v + I_v + W_v$. Based on the expected time scale for the simulation, we exclude H_b and I_b in the definition of n_h since these represent both affected pregnancies and new births that will not interact within the general population in the same way as the other groups. Furthermore, we note that n_h remains constant when $\mu = \alpha = 0$. With initial values given for each population, the solution to system (2.1) can be numerically approximated for a fixed time period, $t \in (0, T]$.

Table 2 gives a list of model parameters and the baseline values we assume in order to illustrate the dynamics of the model and the effectiveness of potential intervention strategies.

Table 2. Description of populations and parameters in the model of Zika dynamics in Figure 1 and Eq 2.1. References for the parameter values are indicated where relevant. Parameters denoted with * were calibrated using parameters from [46] and the analysis of Section 3. All other parameter values are assumed.

Parameter	Baseline values	Definition
p	0.2 [9, 12, 40]	probability of developing symptoms during infection
q_g	0.237 [42]	fraction of women of childbearing age to total pop.
q_m	0.313 [42]	fraction of men age 15–64 to total pop.
e	1/3	effective probability of infection affecting a pregnancy
β_v	0.32 day^{-1} *	vector-to-human transmission rate
β	0.32 day^{-1} *	human-to-vector transmission rate
β_h	0.0055 day^{-1} *	human-to-human transmission rate
β_m	$2\beta_h = 0.011$ day^{-1} *	effective M -to- S transmission rate
κ^{-1}	7 days [9, 39]	mean latency period, human
κ_v^{-1}	10 days [9, 12]	mean latency period, vector
ν^{-1}	10 days [23]	mean duration of infection
γ^{-1}	135 days	mean post-infection pregnancy duration
σ^{-1}	54 days [22, 23]	mean duration of virus survival in semen
θ	4.33×10^{-5} day^{-1} [42]	human birth rate, total pop.
θ_c	1.83×10^{-4} day^{-1} [42]	human birth rate, women of childbearing age
μ	4.33×10^{-5} day^{-1} [42]	human death rate, relative to total pop.
α	8.66×10^{-5} day^{-1}	additional symptomatic death rate
θ_v	1/20 day^{-1} [43, 44]	vector birth rate
μ_v	1/20 day^{-1} [43, 44]	vector death rate
ξ	0.01 day^{-1}	maximum vaccination rate (baseline value $\xi = 0$)

Figure 2 shows the solution of system (2.1) with initial conditions $S(0) = 9990$, $I_s(0) = 2$, $I_a(0) = 8$, $S_v(0) = 9990$, $I_v(0) = 10$, and all other populations at zero initially. We are particularly interested in the final asymptotic value of I_b , which in this example is as follows:

$$\lim_{t \rightarrow \infty} I_b(t) \approx 19.57,$$

which represents the total number of affected pregnancies in the simulated outbreak. The reduction of this value is taken as the primary measure of effectiveness for the intervention strategies studied.

Another way to view the effect of the outbreak on the indicator population is relative to the predicted healthy/unaffected births. This can be done as a cumulative ratio of $I_b(t)$ to the total value of $H_b(t) + I_b(t)$ over time, or as a ratio of the birth rates dI_b/dt to $d(H_b + I_b)/dt$ as a *per day* estimate of the immediate rate of affected births. For the baseline scenario, Figure 3 shows each of these values over time.

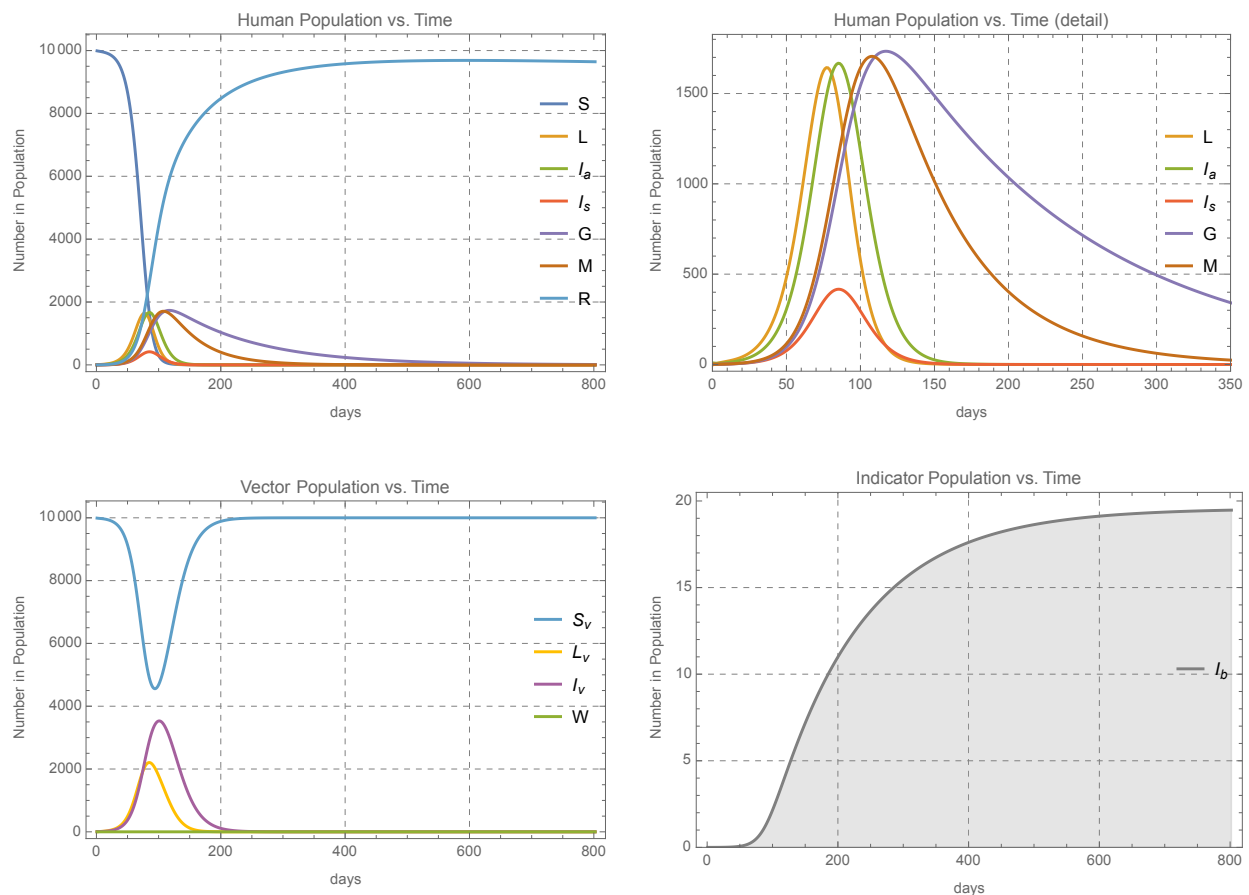


Figure 2. Example of a Zika outbreak with baseline parameters given in Table 2. Human populations are shown in the top row, with the top right plot showing a detail of infected compartments during the active portion of the outbreak. The vector population is shown in the bottom left, and the cumulative number of affected pregnancies as measured by I_b in shown in the bottom right.

As a point of comparison, [47] and [7] describe mechanisms that may help characterize why some pregnancies have severe developmental abnormalities while others do not. The authors of those studies focus on clinical data from Salvador, Brazil following the 2015–2016 outbreak, where

“The clinical results found that approximately 10% of the newborn infants born during the outbreak at the hospital had developed severe birth defects, including microcephaly. [47]”

The results of our model are consistent with this finding, as illustrated in Figure 3. In this scenario, the outbreak subsides by around day 200 and at this point approximately 10.5% of the births are considered affected.

3. Basic reproduction number

The basic reproduction number is a key metric that can help determine the conditions that may lead to the occurrence of an outbreak of a disease. Considering the infected categories $X =$

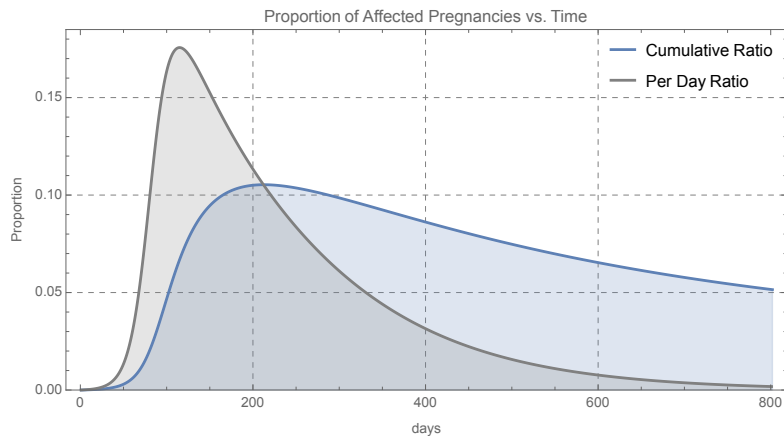


Figure 3. Predicted incidence of affected pregnancies relative to total births.

$(L, I_s, I_a, M, L_v, I_v)$, we use the Next Generation Matrix approach to compute the basic reproduction number for the model (see [48, 49], e.g.). We use the matrix splitting $J = T + \Sigma$, where J is the Jacobian matrix of the system at the disease-free equilibrium with $S = n_h$ and $S_v = n_v$, and T and Σ are the *transmission* and *transition* matrices, respectively. Thus the initial spread of infection is governed by the following:

$$X' = (T + \Sigma)X.$$

To understand the dynamics on a short time scale at the outset of a possible outbreak, we simplify the system by assuming that the human death rates are zero, $\mu = \alpha = 0$, and consider n_h and n_v as constant. This results in

$$T = \begin{pmatrix} 0 & 0 & \beta_h & \beta_m & 0 & \beta_v \frac{n_h}{n_v} \\ 0 & 0 & 0 & 0 & 0 & 0 \\ 0 & 0 & 0 & 0 & 0 & 0 \\ 0 & 0 & 0 & 0 & 0 & 0 \\ 0 & \beta_v \frac{n_v}{n_h} & \beta_v \frac{n_v}{n_h} & 0 & 0 & 0 \\ 0 & 0 & 0 & 0 & 0 & 0 \end{pmatrix}, \text{ and } \Sigma = \begin{pmatrix} -\kappa & 0 & 0 & 0 & 0 & 0 \\ p\kappa & -\nu & 0 & 0 & 0 & 0 \\ (1-p)\kappa & 0 & -\nu & 0 & 0 & 0 \\ 0 & \nu q_m & \nu q_m & -\sigma & 0 & 0 \\ 0 & 0 & 0 & 0 & -(\kappa_v + \mu_v) & 0 \\ 0 & 0 & 0 & 0 & \kappa_v & -\mu_v \end{pmatrix},$$

and the next-generation matrix is given by $K = -T\Sigma^{-1}$. The overall basic reproduction number \mathcal{R}_0 is the spectral radius of K ,

$$\mathcal{R}_0 = \frac{\beta_h(1-p)}{2\nu} + \frac{\beta_m q_m}{2\sigma} + \sqrt{\left(\frac{\beta_h(1-p)}{2\nu} + \frac{\beta_m q_m}{2\sigma}\right)^2 + \frac{\beta\beta_v \kappa_v}{\nu\mu_v(\kappa_v + \mu_v)}}. \quad (3.1)$$

This expression can be decoupled into components that reflect only sexual transmission ($\beta = \beta_v = 0$) or only human-vector transmission ($\beta_h = \beta_m = 0$), given by

$$\mathcal{R}_{0,hh} = \frac{\beta_h(1-p)}{\nu} + \frac{\beta_m q_m}{\sigma} \quad \text{and} \quad \mathcal{R}_{0,hv} = \sqrt{\frac{\beta\beta_v \kappa_v}{\nu\mu_v(\kappa_v + \mu_v)}},$$

respectively. With this determination on the basic reproduction number, we choose the interaction parameters β , β_v , β_h , and β_m to calibrate our model relative to a well-documented recent outbreak.

The study in [46] estimated the basic reproduction number for Barranquilla, Colombia in the 2015 outbreak, which reported an overall value of the reproduction number of 3.8 and the component due to sexual transmission of 0.23.

We take $\beta = \beta_v$, which represents a mosquito/human interaction rate with an equal likelihood of transmission of the virus between humans and mosquitoes, given a bite. Additionally we assume that $\beta_m = 2\beta_h$ since sexual transmission is via semen and that interactions between individuals in the M and S categories necessarily involves an infected male. By comparison, roughly half of the interactions between S and either I_a or I_s will involve an infected male. Under these model assumptions, setting $\mathcal{R}_0 = 3.8$ and $\mathcal{R}_{0,hh} = 0.23$ uniquely determines the interaction parameter values of the following:

$$\beta = \beta_v = 0.32 \text{ day}^{-1} \text{ and } \beta_h = 0.5\beta_m = 0.0055 \text{ day}^{-1}.$$

Additionally, this yields a basic reproduction value of $\mathcal{R}_{0,hv} = 3.7$ for purely human-vector transmission. As expected, in an acute outbreak, transmission is dominated by human-vector contact.

Another natural question to consider is the threshold for herd immunity, either through recovery or vaccination. Considering only human-vector interaction, we define the herd immunity threshold (HIT) as the minimum fraction of the initial S population that must be immune to achieve an effective $\mathcal{R}_{0,hv} \leq 1$.

Linearizing the system about $S = (1 - \text{HIT})n_h$, $R = \text{HIT } n_h$, and $S_v = n_v$, the next-generation matrix method results in a modified reproduction ratio of

$$\mathcal{R}_{0,hv} = \sqrt{\frac{(1 - \text{HIT})\beta\beta_v\kappa_v}{\nu\mu_v(\kappa_v + \mu_v)}}.$$

Setting $\mathcal{R}_{0,hv} < 1$ and solving for HIT results in a threshold of

$$\text{HIT} = 1 - \frac{\nu\mu_v(\kappa_v + \mu_v)}{\beta\beta_v\kappa_v}. \quad (3.2)$$

Using the parameter values in Table 2, we find a value of $\text{HIT} = 0.929$. Here, we note that this analysis assumes an initial fully susceptible vector population, $S_v \approx n_v$. This results in a relatively high value for the HIT since the initial immunity is only assumed for the human susceptible population.

4. Wolbachia as a control mechanism

In this section, we illustrate the dynamics and potential effectiveness of introducing Wolbachia-infected mosquitoes as a control mechanism to reduce the spread of infectious diseases such as Zika, dengue, chikungunya, and yellow fever. The overall goal of the World Mosquito Program is to create endemic populations of Wolbachia-infected mosquitoes as a way of keeping a mosquito-borne infection below an epidemic threshold. Since the presence of Wolbachia in the gut of infected mosquitoes prevents the replication of Zika [45], this program is analogous to a vaccination routine in a human population. As such, in the same way that an effective vaccine for humans can create a threshold of herd immunity, a significant level of Wolbachia-infected mosquitoes can ensure that the basic reproduction number remains below unity. With analogous reasoning to a vaccine induced herd immunity, we define

the Wolbachia immunity threshold (WIT) as the minimum fraction of the total vector population for W_v to achieve an effective $\mathcal{R}_{0,hv} \leq 1$. As in Section 3, this results in the following:

$$\text{WIT} = 1 - \frac{\nu\mu_v(\kappa_v + \mu_v)}{\beta\beta_v\kappa_v}, \quad (4.1)$$

which is the same as the threshold value for the HIT. Thus, in our baseline scenario, achieving a level of 93% Wolbachia-infected mosquitoes is sufficient to keep the system below the epidemic threshold.

To understand the dynamics related to Wolbachia, we assume an initial disease-free state, where the vector populations S_v and W_v are decoupled from the full system. This simplified model is illustrated in Figure 4.

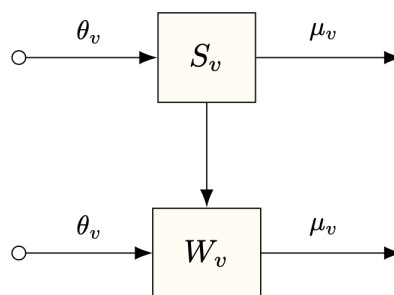


Figure 4. Compartment vector model in a disease-free state.

The corresponding dynamics are governed by system (4.2). To illustrate, we note that this model is calibrated so that when $S_v = W_v = n_v/2$ the emergence rate into W_v is twice the rate into S_v , which is consistent with the reproduction dynamics of cohabitating populations of Wolbachia-infected and native mosquitoes as described in Section 2. The resulting coupled ODE is given by the following:

$$\begin{aligned} \frac{dS_v}{dt} &= \theta_v \left(1 - \frac{2W_v}{3n_v} \right) S_v - \mu_v S_v, & S_v(0) &= (1-r)n_v, \\ \frac{dW_v}{dt} &= \theta_v \left(1 + \frac{2S_v}{3n_v} \right) W_v - \mu_v W_v, & W_v(0) &= rn_v, \end{aligned} \quad (4.2)$$

where the parameter $r \in [0, 1]$ in the initial conditions indicates the fraction of the total mosquito population that is infected with Wolbachia. Assuming equal birth and death rates, $n_v = S_v + W_v$ is constant in time, and (4.2) easily decouples to two logistic ODEs:

$$\begin{aligned} \frac{dS_v}{dt} &= -\frac{2\theta_v}{3n_v} S_v (n_v - S_v), & \text{and} & & \frac{dW_v}{dt} &= \frac{2\theta_v}{3n_v} W_v (n_v - W_v), \\ S_v(0) &= (1-r)n_v, & & & W_v(0) &= rn_v. \end{aligned}$$

The initial conditions for S_v and W_v show the relative scale of the release of Wolbachia-infected mosquitoes into a susceptible population, and the corresponding solutions for $S_v(t)$ and $W_v(t)$ reveal the time scale for which Wolbachia can be considered endemic to a region. Figure 5 illustrates the growth of W_v over time using $\theta_v = \mu_v = 1/20 \text{ day}^{-1}$.

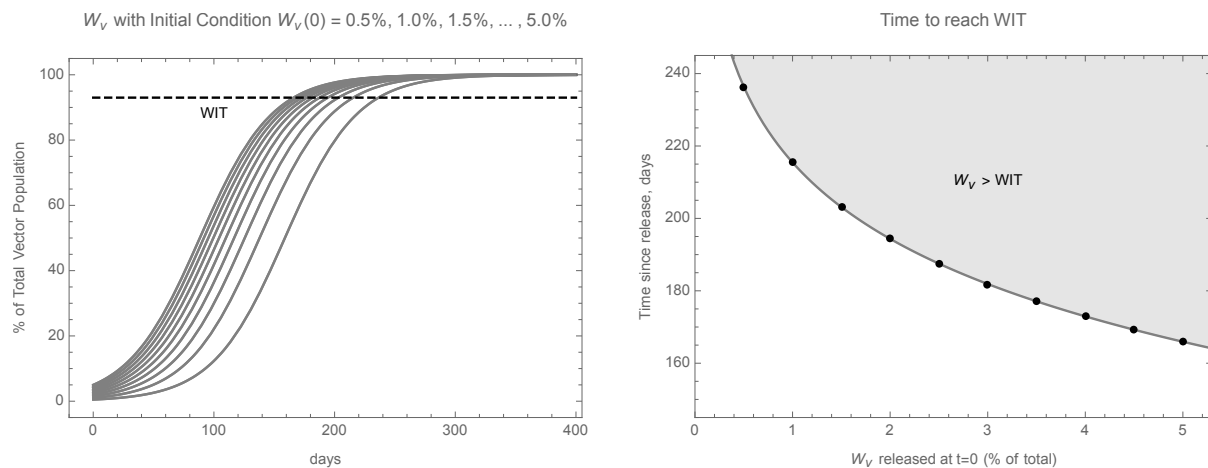


Figure 5. Replacement dynamics of Wolbachia-infected mosquito population in a disease-free environment with equal vector birth and death rates. Proportion of Wolbachia-infected mosquitoes after introducing W_v at 0.5–5% of the total vector population (left), and the corresponding times to reach the immunity threshold WIT (right).

This shows that introducing Wolbachia-infected mosquitoes at 0.5–5% of the total vector population will reach the $WIT \approx 93\%$ threshold in approximately 165–240 days. This time scale predicted by our model is consistent with results found in [50], where staged releases of Wolbachia-infected mosquitoes reached similar endemic levels within approximately 9–12 months on average across 12 intervention clusters near Yogyakarta, Indonesia. In that study, after the introduction period, Wolbachia prevalence remained near 100% in the geographic regions treated. If mosquitoes infected with Wolbachia have a high level of resistance to transmitting Zika in the wild, then this evidence suggests that Wolbachia could provide an effective and durable protection against regional Zika outbreaks.

Additionally, we see good agreement in the overall timescale for Wolbachia spread as predicted by more detailed mathematical models, such as in [34], where a hierarchy of models consistently showed Wolbachia replacement in approximately 200 days. While it is possible to segment the mosquito population to separately model sex or age distinctions as in this study, we find that our model effectively captures the key elements most relevant to the Zika/Wolbachia dynamic.

Moreover, it is worth noting that the time scale for replacement is likely too long for Wolbachia to be effective as a control measure when an outbreak is beginning. To illustrate this, Figure 6 shows the vector population in the baseline scenario compared with the initial introduction of W_v at 1% of the total vector population. Here, Wolbachia replacement only marginally decreases the overall spread of Zika. In this scenario, the most active period of virus transmission occurs in the 50–100 day range, while W_v doesn't reach the immunity threshold until approximately 200 days. Under this scenario, the number of affected pregnancies is essentially unchanged from the baseline scenario.

In the next section, we consider several intervention strategies that are better candidates for controlling an outbreak as it occurs.

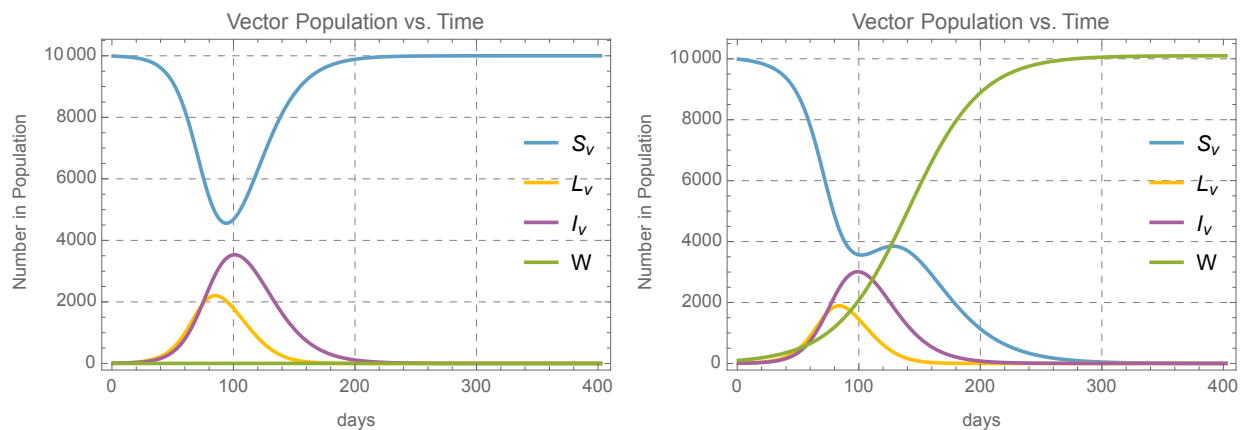


Figure 6. Vector populations in the baseline outbreak simulation with no Wolbachia presence (left) compared with the initial introduction of W_v at 1% of the total vector population.

5. Modified model with intervention strategies

We consider six intervention strategies with the potential to reduce the number of affected pregnancies predicted by the model. Each intervention is parameterized by a unitless control variable as described below:

- Reduce the human-vector contact rate by the proportion $0.25 \leq c_1 \leq 1$. Public health awareness campaigns to encourage people to avoid or reduce contact with mosquitoes can have this effect (e.g., using bed nets, mosquito repellents, etc.). This results in the replacement

$$\beta \rightarrow c_1\beta \text{ and } \beta_v \rightarrow c_1\beta_v$$

in Eqs 1, 2, 8, and 9 of system (2.1). For example, a value of $c_1 = 0.25$ would represent a reduction of human-vector contact to 25% of the baseline value.

- Reduce the human-human contact rate by the proportion $0.25 \leq c_2 \leq 1$, which reduces the parameters β_h and β_m . Public health awareness campaigns to encourage people to avoid unprotected sexual contact with potentially infected individuals can have this effect. This results in the replacement

$$\beta_h \rightarrow c_2\beta_h \text{ and } \beta_m \rightarrow c_2\beta_m$$

in the first two equations of system (2.1).

- Increase the natural mosquito death rate by a factor of $1 \leq c_3 \leq 8$, which increases the parameter μ_v . Mosquito adulticide efforts can have this effect. This results in the replacement

$$\mu_v \rightarrow c_3\mu_v$$

in Eqs 8–10 of system (2.1). For example, a value of $c_3 = 8$ would indicate increasing the death rate of the mosquito population to 8 times the natural rate.

- Decrease the mosquito emergence rate by a factor of $0.25 \leq c_4 \leq 1$, which reduces the parameter θ_v . Treatment of stagnant water sources and mosquito larvacide efforts can have this effect. This results in the replacement

$$\theta_v \rightarrow c_4 \theta_v$$

in Eqs 8 and 11 of system (2.1). For example, a value of $c_4 = 0.25$ would reflect reducing the emergence rate to 25% of the natural emergence rate.

- Vaccinate susceptible people at a rate of up to $\xi = 0.01 \text{ day}^{-1}$ starting from $t = 0$. The modified model assumes a transition from S to R with a rate of $(1 - c_5)\xi$, where $(1 - c_5) \leq 1$ represents the fraction of the maximum rate of 1% of the population vaccinated per day, with $0 \leq c_5 \leq 1$. A value of $c_5 = 1$ represents no vaccination, while a value of $c_5 = 0$ represents vaccinating 1% of the population per day. This assumes the existence of a vaccine that is fully effective upon administration, and we assume that vaccination will change a susceptible person to the recovered category, while vaccination of those in other populations will not result in a category change.
- Start the simulation with a proportion of the susceptible population already vaccinated. This is implemented by taking the initial conditions $S(0) = c_6 S_0$ and $R(0) = R_0 + (1 - c_6)S_0$ with $c_6 \leq 1$ for $0.5 \leq c_6 \leq 1$. This assumes the existence of a fully effective vaccine in place as a preventative measure before the emergence of a potential outbreak.

Each of these control variables are defined so that $c_i = 1$ ($i = 1, 2, \dots, 6$) corresponds to the baseline situation with no interventions implemented.

6. Control variable sensitivity analysis

In this section, we study the overall effectiveness and sensitivity of each of the six control parameters in predicting the total number of affected pregnancies in the course of an outbreak. Table 3 gives the assumed range of each control parameter and the corresponding ranges for the associated model parameters. Using the baseline model parameters in Table 2, the maximum asymptotic value of I_b is approximately 19.57, as illustrated in Section 2 above.

Table 3. Control parameter ranges and corresponding model parameter ranges. The control parameters are dimensionless, and a value of 1 represents no intervention implementation. For the model parameters and definitions, see Table 2.

Parameter	Min	Max	Corresponding parameter range
c_1	0.25	1.0	$\beta, \beta_v \in [0.08, 0.32] \text{ day}^{-1}$
c_2	0.25	1.0	$\beta_h \in [0.001375, 0.0055] \text{ day}^{-1}, \beta_m \in [0.00275, 0.011] \text{ day}^{-1}$
c_3	1.0	8.0	$\mu_v \in [0.0333, 0.267] \text{ day}^{-1}$
c_4	0.25	1.0	$\theta_v \in [0.0125, 0.05] \text{ day}^{-1}$
c_5	0	1.0	$\xi \in [0, 0.01] \text{ day}^{-1}$
c_6	0.5	1.0	Vaccinate 0–50% of the initial S population before $t = 0$

First we consider the implementation of each control strategy in isolation. Figure 7 shows the relationship between the asymptotic value of I_b and c_i , $i = 1, 2, \dots, 6$, where $c_j = 1$ for $j \neq i$.

In this context, it is clear that only the two vaccination strategies, c_5 and c_6 , have an immediate effect in the absence of other interventions. This can be taken as an encouraging sign of the effectiveness of potential vaccination efforts in reducing the number of affected pregnancies, either as a just-in-time intervention or to be applied as a population-wide protection in a region susceptible to future outbreaks.

Additionally, we see that reducing the human-human sexual contact, c_2 , and reducing the vector birth rate, c_4 , have very little effect in this regime. Reducing the human-vector contact, c_1 , and increasing the vector death rate, c_3 , have significant effects, but only when applied beyond a threshold. This preliminary *local* analysis is helpful in determining the marginal benefit of the controls.

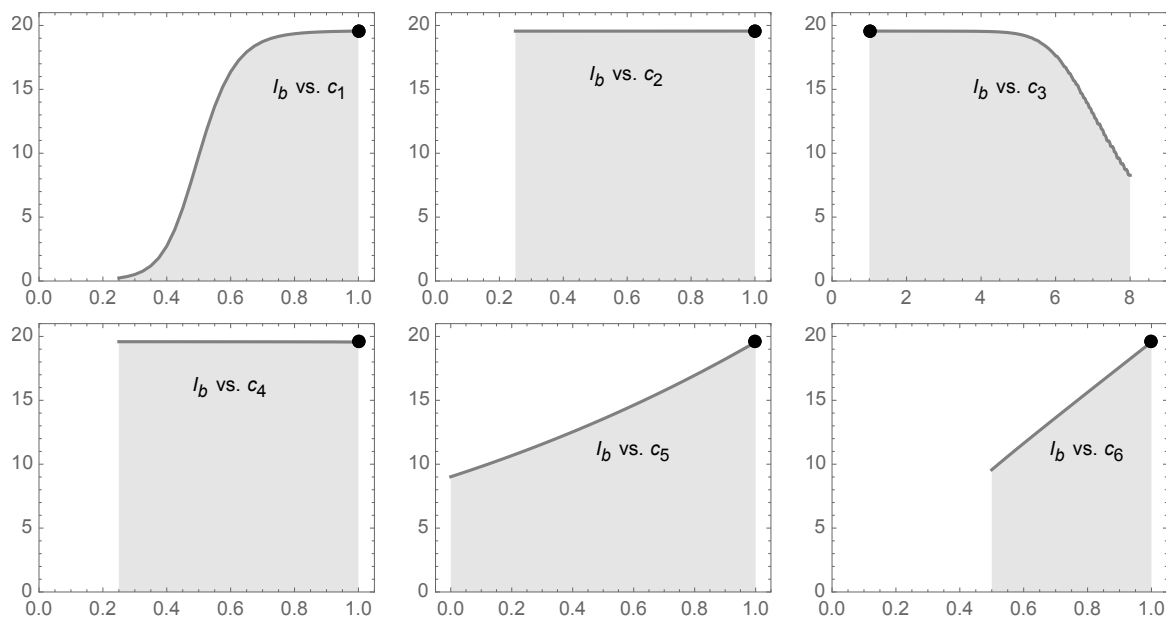


Figure 7. Indicator population sensitivity response to individual control parameter values. Plots of I_b vs. c_i are shown for the parameter values in Table 3 for $i = 1, 2, \dots, 6$, and the baseline value of $c_i = 1$ is shown with a single point.

A more *global* view of parameter sensitivity is found through a Latin Hypercube Sampling and Partial Rank Correlation Coefficient (LHS/PRCC) method [51]. We assume a uniform distribution of values for c_i , $i = 1, 2, \dots, 6$, in the ranges described in Table 3, and use a LHS of $N = 5000$ values. For each combination of parameter values, we simulate the system for $t \leq T = 1000$ days and compute the asymptotic value of I_b . With this data PRCC values are computed to estimate the sensitivity of I_b to each variable, while taking the effect of the other variables into account. Scatter plots of the residual ranking are shown in Figure 8, and the corresponding PRCC values are shown in Figure 9. While all six parameters are nonzero with statistical significance at the $p = 0.005$ level, there is a clear distinction between the most and least influential intervention strategies.

As a primarily vector-borne disease, it is intuitive that reducing the human-mosquito interaction rate (i.e., decreasing c_1) has a large effect. Reducing the sexual contact rate between human populations (decreasing c_2) has the smallest effect overall. This contrast is consistent with the findings that the

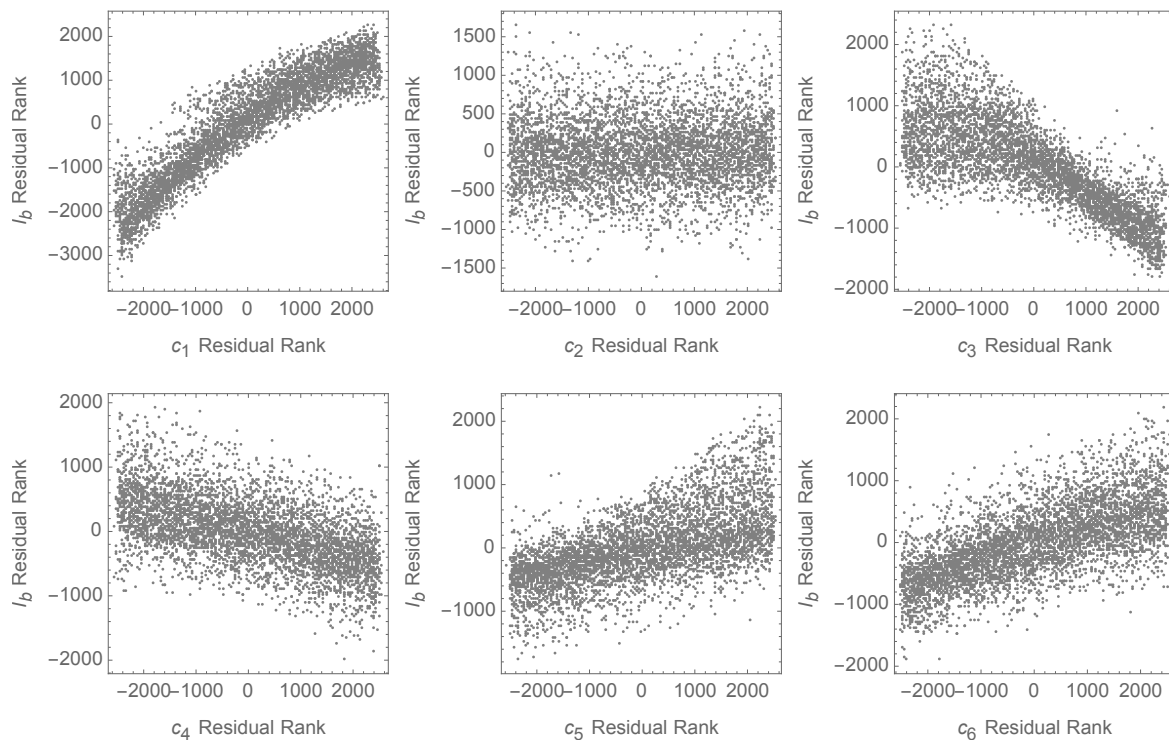


Figure 8. Scatter plots of simulated data for the PRCC analysis, $N = 5000$ values.

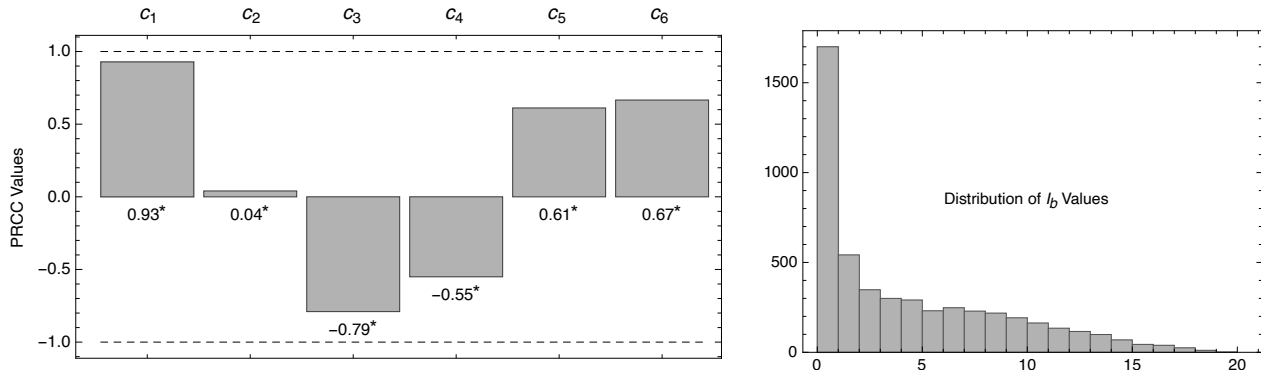


Figure 9. PRCC analysis based on the asymptotic value of I_b for each control variable, $N = 5000$ samples. PRCC values (left) and distribution of I_b values (right). * Indicates the value is non-zero with statistical significance, $p\text{-value} \leq 0.005$.

basic reproduction number is dominated by human-vector interaction.

Additionally, the results show an interesting difference in the sensitivity related to modifying either the vector death or birth rates. Accelerating the mosquito death rate (increasing c_3) can result in a significant reduction on the number of affected pregnancies. However, lower values of the mosquito birth rate, on average, correspond to slightly higher affected pregnancy values. While this seems counterintuitive, a typical simulated outbreak occurs on a relatively short time scale, where most of the critical transmission between the human-vector populations occurs as a result of the initial existing

adult mosquito population. Decreasing the emergence of new non-infected mosquitoes in subsequent generations serves to increase the proportion of infected mosquitoes (i.e., I_v/n_v) during the part of the critical time for transmissions.

The final two control parameters relate to the use of an effective vaccine. Both methods, administering a vaccine at a faster rate through an outbreak (i.e., larger c_5 values) and beginning a potential outbreak with a higher proportion of vaccinated people (i.e., larger c_6 values), have a significant impact on the number of affected births. Each of these approaches tend to give benefits that are directly proportional to the level of intervention. This finding directly supports the public health value of vaccination at any level, should a vaccine become available.

7. Sexual transmission of Zika

While the role of sexual transmission of Zika virus is still not well-understood, it is expected to play an important role in the broad context of Zika dynamics (e.g., see [17]). In this section, we examine the potential scope of sexual human-human transmission, independent of the more dominant human-vector routes. In particular, we consider the relevant time scales when the persistence of a transmissible virus in the semen of infected males may be longer than the typical lifespan of mosquitoes.

Furthermore, we recall that the use of population-level statistics and compartmental models both assume homogenous and well-mixed populations. In reality, the transmission rate parameters may widely vary in different sub-population clusters. As such, in subsets of the population with high rates of sexual activity, it may be possible for virus transmission to persist, in essence as a sexually transmitted infection [20]. In this framework, sexual transmission may contribute to Zika becoming regionally endemic, even if it plays a less important role on the timescale of an epidemic.

In Section 3, we used population level data to estimate the transmission parameters β , β_v , β_h , and β_m . These represent the average rates of human-vector and human-human interactions. In the range of values assumed in Table 3, our model predicts that the human-vector interaction rate is much more significant than the human-human interaction rate. While this is likely accurate in the context of an active epidemic, we consider the component of sexual transmission only, which may exist in the absence of vector transmission. Assuming no human-vector interaction, $\beta = \beta_v = 0$, the basic reproduction number simplifies to the following:

$$\mathcal{R}_0 = \mathcal{R}_{0,hh} = \frac{\beta_h(1-p)}{\nu} + \frac{2\beta_h q_m}{\sigma}.$$

Under the same assumptions and values for ν , σ , p , and q_m as in Section 2, we find that $\mathcal{R}_{0,hh} > 1$ when

$$\beta_h > \frac{\nu\sigma}{(1-p)\sigma + 2q_m\nu} \approx 0.024 \text{ day}^{-1}$$

Within subsets of the general population that have high rates of sexual activity, it is reasonable to assume the possibility of interaction rates exceeding this value. To illustrate the potential time scales associated with a sexually transmitted Zika epidemic, we take values $\beta_h = 0.036$ and 0.060 day^{-1} , which correspond to $\mathcal{R}_{0,hh} = 1.5$ and 2.5 . Additionally, we take $\beta = \beta_v = 0$, $\beta_m = 2\beta_h$ and all other parameters as in 2. Figure 10 shows the resulting epidemic in a population of 10,000 people, assuming the initial conditions $S(0) = 9990$, $I_s(0) = 2$, and $I_a(0) = 8$.

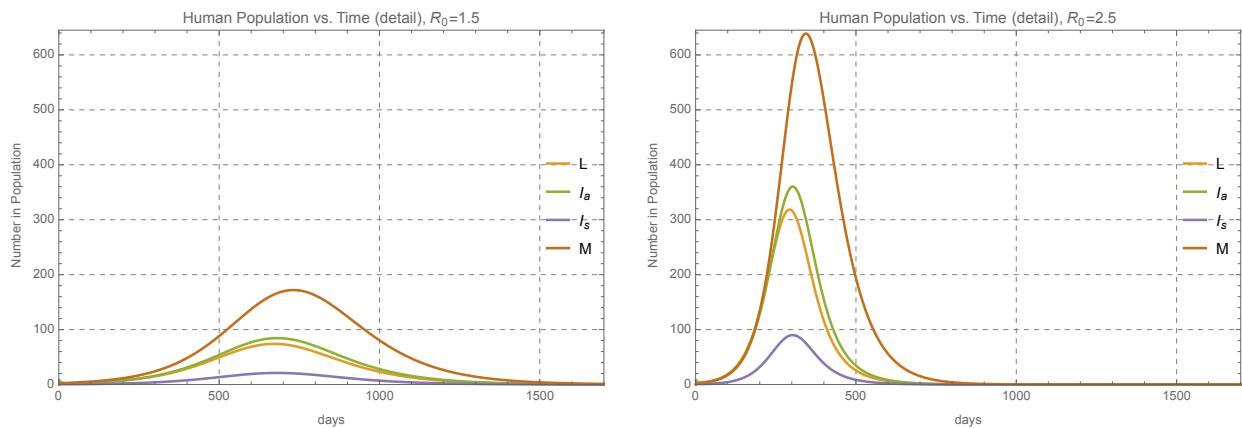


Figure 10. Zika Sexual transmission in human populations with $\beta_h = 0.036$ and 0.060 day^{-1} , which corresponds to $\mathcal{R}_0 = \mathcal{R}_{0,hh} = 1.5$ and 2.5 .

We see that the time scale for a sexually transmitted epidemic is much longer than one driven primarily by human-vector interaction. While there is no evidence that such epidemics have occurred [21], this does illustrate the possibility that sexually active human males may provide a reservoir for Zika virus. This may have implications for understanding how Zika spreads into new geographic regions or how Zika may persist in endemic regions over times where the mosquito populations are less active. This idea was explored in [18] through a network based epidemic model. That study showed conditions for which a Zika outbreak was sustained for up to three months in a sexual contact network in the absence of mosquito contact. Likewise, [15] used sexual contact network models and found that sub-populations of men-who-have-sex-with-men (MSM) have a greatly increased likelihood of sustaining Zika above a localized epidemic threshold. This is a dynamic that the authors identified as overlooked by traditional epidemiological surveillance methods. The existence of separate contact networks and time scales for human-human and human-vector interactions could help explain the transition into an endemic state where mosquito activity is seasonal.

8. Discussion and conclusions

Zika outbreaks have the potential to adversely affect a significant number of pregnancies, and it is important to understand the dynamics of the disease transmission and the relative merits of different control strategies. The compartmental model proposed in this paper provides a mechanism to evaluate the potential effectiveness of traditional public health intervention methods as well as the use of vaccines and novel approaches such as the use of Wolbachia-infected mosquitoes.

Zika virus spreads as a vector-borne disease through human-mosquito contact as well as through human-human sexual contact. To understand the dynamics relative to these dual transmission routes the overall basic reproduction number is decomposed into human-mosquito and human-human components. Additionally, we demonstrate that these transmission pathways have significantly different timescales.

Our approach characterizes the sensitivity of the model to the number of affected pregnancies, which

is the primary concern with this disease. Our model predicts the rates of developmental abnormalities consistent with known Zika outbreaks and provides a framework to study interventions that have the most impact on reducing the affected pregnancies.

Our analysis shows that, if a Wolbachia infection effectively blocks Zika transmission, then a region can reach an immunity threshold within approximately 200 days after an initial release. Additionally, we find that this time scale is too long for a Wolbachia release to be effective in combating a Zika outbreak that is just beginning. Thus, we find that Wolbachia releases have an additional potential to protect a region pre-epidemic than using it as a just-in-time intervention.

Interventions that may be used in addressing an epidemic in the initial stages of an outbreak are often considered in the context of limited resources. Our analysis of six control mechanisms show that reducing human-mosquito contact and decreasing the adult mosquito population are the two most effective measures studied.

Moreover, our model admits an examination of the herd immunity threshold. We find that under conditions similar to the 2015 outbreak in Colombia, Zika will remain below the epidemic threshold when approximately 93% of the human population is immune because of either prior infection or vaccination. Though achieving this value in practice seems daunting, we find that reducing the susceptible population before an outbreak has an immediate and proportional reduction in the predicted number of affected pregnancies. For example, if 10% of the population is immune, then an epidemic will still occur, but the number of affected pregnancies will be reduced by approximately 10%. Thus, should a vaccine become available, it has the potential to be an important tool in reducing the number of Zika-affected pregnancies, even if it does not fully prevent an outbreak.

Additionally, this model allows the study of sexual spread of Zika virus as a component of the overall transmission dynamics. While the human-mosquito transmission is the dominant pathway for a typical outbreak modeled here, it is certainly possible for subsets of the human population to maintain sexual contact rates above the epidemic threshold. We anticipate that the role of sexual transmission of Zika will continue to be an important key to understanding the complex nature of how Zika outbreaks emerge.

Use of AI tools declaration

The authors declare they have not used Artificial Intelligence (AI) tools in the creation of this article.

Conflict of interest

The authors declare there is no conflict of interest.

Disclaimer

The views expressed in this article, book, or presentation are those of the author and do not necessarily reflect the official policy or position of the United States Air Force Academy, the Air Force, the Department of Defense, or the U.S. Government. Approved for public release: distribution unlimited. PA # USAFA-DF-2025-229.

References

1. R. Lowe, C. Barcellos, P. Brasil, O. G. Cruz, N. A. Honório, H. Kuper, et al., The Zika virus epidemic in Brazil: from discovery to future implications, *Int. J. Environ. Res. Public Health*, **15** (2018), 96. <https://doi.org/10.3390/ijerph15010096>
2. O. Pacheco, M. Beltrán, C. A. Nelson, D. Valencia, N. Tolosa, S. L. Farr, et al., Zika virus disease in Colombia—preliminary report, *N. Engl. J. Med.*, **383** (2020), e44. <https://doi.org/10.1056/NEJMoa1604037>
3. L. H. Chen, D. H. Hamer, Zika virus: Rapid spread in the western hemisphere, *Ann. Intern. Med.*, **64** (2016), 613–615. <https://doi.org/10.7326/M16-0150>
4. W. K. Oliveira, G. V. A. de França, E. H. Carmo, B. B. Duncan, R. S. Kuchenbecker, M. I. Schmidt, Infection-related microcephaly after the 2015 and 2016 Zika virus outbreaks in Brazil: a surveillance-based analysis, *Lancet*, **390** (2017), 861–870. [https://doi.org/10.1016/S0140-6736\(17\)31368-5](https://doi.org/10.1016/S0140-6736(17)31368-5)
5. S. R. Ellington, O. Devine, J. Bertolli, A. M. Quiñones, C. K. Shapiro-Mendoza, J. Perez-Padilla, et al., Estimating the number of pregnant women infected with Zika virus and expected infants with microcephaly following the Zika virus outbreak in Puerto Rico, 2016, *JAMA Pediatr.*, **170** (2016), 940–945. <https://doi.org/10.1001/jamapediatrics.2016.2974>
6. M. L. Ospina, V. T. Tong, M. Gonzalez, D. Valencia, M. Mercado, S. M. Gilboa, et al., Zika virus disease and pregnancy outcomes in Colombia, *N. Engl. J. Med.*, **383** (2020), 537–545. <https://doi.org/10.1056/NEJMoa1911023>
7. D. F. Robbiani, P. C. Olsen, F. Costa, Q. Wang, T. Y. Oliveira, N. Nery Jr, et al., Risk of Zika microcephaly correlates with features of maternal antibodies, *J. Exp. Med.*, **216** (2019), 2302–2315. <https://doi.org/10.1084/jem.20191061>
8. L. T. Keegan, J. Lessler, M. A. Johansson, Quantifying Zika: Advancing the epidemiology of Zika with quantitative models, *J. Infect. Dis.*, **216** (2017), S884–S890. <https://doi.org/10.1093/infdis/jix437>
9. V. C. Agumadu, K. Ramphul, Zika virus: A review of literature, *Asian Pac. J. Trop. Biomed.*, **6** (2016), 989–994. <https://doi.org/10.7759/cureus.3025>
10. A. A. Momoh, A. Fügenschuh, Optimal control of intervention strategies and cost effectiveness analysis for a Zika virus model, *Oper. Res. Health Care*, **18** (2018), 99–111. <https://doi.org/10.1016/j.orhc.2017.08.004>
11. E. Bonyah, K. Okosun, Mathematical modeling of Zika virus, *Asian Pac. J. Trop. Dis.*, **6** (2016), 673–679. [https://doi.org/10.1016/S2222-1808\(16\)61108-8](https://doi.org/10.1016/S2222-1808(16)61108-8)
12. D. Gao, Y. Lou, D. He, T. C. Porco, Y. Kuang, G. Chowell, et al., Prevention and control of Zika as a mosquito-borne and sexually transmitted disease: A mathematical modeling analysis, *Sci. Rep.*, **6** (2016), 28070. <https://doi.org/10.1038/srep28070>
13. D. F. Aranda, G. Gonzalez-Parra, T. Benincasa, Mathematical modeling and numerical simulations of Zika in Colombia considering mutation, *Math. Comput. Simul.*, **163** (2019), 1–18. <https://doi.org/10.1016/j.matcom.2019.02.009>

14. C. L. Althaus, N. Low, How relevant is sexual transmission of Zika virus, *PLOS Med.*, **13** (2016), 1–3. <https://doi.org/10.1371/journal.pmed.1002157>
15. A. Allard, B. M. Althouse, L. Hebert-Dufresne, S. V. Scarpino, The risk of sustained sexual transmission of Zika is underestimated, *PLoS Pathog.*, **13** (2017), 1–12. <https://doi.org/10.1371/journal.ppat.1006633>
16. M. Sherley, C. W. Ong, Sexual transmission of Zika virus: a literature review, *Sex Health*, **15** (2018), 183–199. <https://doi.org/10.1071/SH17046>
17. C. R. Kim, M. Counotte, K. Bernstein, C. Deal, P. Mayaud, N. Low, et al., Investigating the sexual transmission of Zika virus, *Lancet Global Health*, **6** (2018), e24–e25. [https://doi.org/10.1016/S2214-109X\(17\)30419-9](https://doi.org/10.1016/S2214-109X(17)30419-9)
18. T. Ferdousi, L. W. Cohnstaedt, D. S. McVey, C. M. Scoglio, Understanding the survival of Zika virus in a vector interconnected sexual contact network, *Sci. Rep.*, **9** (2019), 7253. <https://doi.org/10.1038/s41598-019-43651-3>
19. B. S. von Essen, K. Kortsmits, L. Warner, D. V. D'Angelo, H. B. Shulman, W. H. Virella, et al., Preventing sexual transmission of Zika virus infection during pregnancy, Puerto Rico, USA, 2016, *Emerg. Infect. Dis.*, **25** (2019), 2115–2119. <https://doi.org/10.3201/eid2511.190915>
20. M. Rodriguez, A. Lord, C. C. Sanabia, A. Silverio, M. Chuang, S. M. Dolan, Understanding Zika virus as an STI: findings from a qualitative study of pregnant women in the Bronx, *Sex. Transm. Infect.*, **96** (2020), 80–84. <https://doi.org/10.1136/sextrans-2019-054093>
21. C. G. Major, G. Paz-Bailey, S. L. Hills, D. M. Rodriguez, B. J. Biggerstaff, M. Johansson, Risk estimation of sexual transmission of Zika virus—United States, 2016–2017, *J. Infect. Dis.*, **224** (2021), 1756–1764. <https://doi.org/10.1093/infdis/jiab173>
22. P. S. Mead, N. K. Duggal, S. A. Hook, M. Delorey, M. Fischer, D. Olzenak McGuire, et al., Zika virus shedding in semen of symptomatic infected men, *N. Engl. J. Med.*, **378** (2018), 1377–1385. <https://doi.org/10.1056/NEJMoa1711038>
23. F. A. Medina, G. Torres, J. Acevedo, S. Fonseca, L. Casiano, C. M. De León-Rodríguez, et al., Duration of the presence of infectious Zika virus in semen and serum, *J. Infect. Dis.*, **219** (2019), 31–40. <https://doi.org/10.1093/infdis/jiy462>
24. M. Izquierdo-Suzán, S. Zárate, J. Torres-Flores, F. Correa-Morales, C. González-Acosta, E. E. Sevilla-Reyes, et al., Natural vertical transmission of Zika virus in larval *Aedes aegypti* populations, Morelos, Mexico, *Emerg. Infect. Dis.*, **25** (2019), 1477–1484. <https://doi.org/10.3201/eid2508.181533>
25. M. A. Ibrahim, A. Dénes, Threshold dynamics in a model for Zika virus disease with seasonality, *Bull. Math. Biol.*, **83** (2021), 27. <https://doi.org/10.1007/s11538-020-00844-6>
26. A. Srivastav, J. Yang, X. F. Luo, M. Ghosh, Spread of Zika virus disease on complex network—a mathematical study, *Math. Comput. Simul.*, **157** (2019), 15–38. <https://doi.org/10.1016/j.matcom.2018.09.014>
27. S. L. Li, J. P. Messina, O. G. Pybus, M. U. G. Kraemer, L. Gardner, A review of models applied to the geographic spread of Zika virus, *Trans. R. Soc. Trop. Med. Hyg.*, **115** (2021), 956–964. <https://doi.org/10.1093/trstmh/trab009>

28. U. A. Danbaba, S. M. Garba, Modeling the transmission dynamics of Zika with sterile insect technique, *Math. Methods Appl. Sci.*, **41** (2018), 8871–8896. <https://doi.org/10.1002/mma.5336>
29. M. N. Rocha, M. M. Duarte, S. B. Mansur, B. D. M. e Silva, T. N. Pereira, T. é. R. Adelino, et al., Pluripotency of Wolbachia against arboviruses: the case of yellow fever, *Gates Open Res.*, **3** (2019), 161. <https://doi.org/10.12688/gatesopenres.12903.2>
30. C. Indriani, W. Tantowijoyo, E. Rancès, B. Andari, E. Prabowo, D. Yusdi, et al., Reduced dengue incidence following deployments of Wolbachia-infected *Aedes aegypti* in Yogyakarta, Indonesia: a quasi-experimental trial using controlled interrupted time series analysis, *Gates Open Res.*, **4** (2020), 50. <https://doi.org/10.12688/gatesopenres.13122.1>
31. S. B. Pinto, T. I. S. Riback, G. Sylvestre, G. Costa, J. Peixoto, F. B. S. Dias, et al., Effectiveness of Wolbachia-infected mosquito deployments in reducing the incidence of dengue and other Aedes-borne diseases in Niterói, Brazil: A quasi-experimental study, *PLoS Negl. Trop. Dis.*, **15** (2021), e0009556. <https://doi.org/10.1371/journal.pntd.0009556>
32. L. Wang, H. Zhao, S. M. Oliva, H. Zhu, Modeling the transmission and control of Zika in Brazil, *Sci. Rep.*, **7** (2017), 7721. <https://doi.org/10.1038/s41598-017-07264-y>
33. L. Xue, X. Cao, H. Wan, Releasing Wolbachia-infected mosquitos to mitigate the transmission of Zika virus, journal of mathematical analysis and applications, *J. Math. Anal. Appl.*, **496** (2021), 27. <https://doi.org/10.1016/j.jmaa.2020.124804>
34. Z. Qu, J. M. Hyman, Generating a hierarchy of reduced models for a system of differential equations modeling the spread of Wolbachia in mosquitoes, *SIAM J. Appl. Math.*, **79** (2019), 1675–1699. <https://doi.org/10.1137/19M1250054>
35. P. M. S. Castanha, E. T. A. Marques, A glimmer of hope: Recent updates and future challenges in Zika vaccine development, *Viruses*, **12** (2020), 1371. <https://doi.org/10.3390/v12121371>
36. S. E. Woodson, K. M. Morabito, Continuing development of vaccines and monoclonal antibodies against Zika virus, *npj Vaccines*, **9** (2024), 91. <https://doi.org/10.1038/s41541-024-00889-x>
37. W. Valega-Mackenzie, K. Ríos-Soto, Can vaccination save a Zika virus epidemic, *Bull. Math. Biol.*, **80** (2018), 598–625. <https://doi.org/10.1007/s11538-018-0393-7>
38. T. Y. Miyaoka, S. Lenhart, J. F. C. A. Meyer, Optimal control of vaccination in a vector-borne reaction-diffusion model applied to Zika virus, *J. Math. Biol.*, **79** (2019), 1077–1104. <https://doi.org/10.1007/s00285-019-01390-z>
39. E. R. Krow-Lucal, B. J. Biggerstaff, J. E. Staples, Estimated incubation period for Zika virus disease, *Emerg. Infect. Dis.*, **23** (2017), 841–845. <https://doi.org/10.3201/eid2305.161715>
40. M. R. Duffy, T. H. Chen, W. T. Hancock, A. M. Powers, J. L. Kool, R. S. Lanciotti, et al., Zika virus outbreak on Yap Island, Federated States of Micronesia, *N. Engl. J. Med.*, **360** (2009), 2536–2543. <https://doi.org/10.1056/NEJMoa0805715>
41. M. M. Haby, M. Pinart, V. Elias, L. Reveiz, Prevalence of asymptomatic Zika virus infection: a systematic review, *Bull. World Health Organ.*, **96** (2018), 402–413D. <https://doi.org/10.2471/BLT.17.201541>

42. National Administrative Department of Statistics (DANE) (Colombia), *Colombia Population and Housing Census 2018*, 2018. Available from: <https://ghdx.healthdata.org/record/colombia-population-and-housing-census-2018>.
43. L. M. Rueda, K. J. Patel, R. C. Axtell, R. E. Stinner, Temperature-dependent development and survival rates of *Culex quinquefasciatus* and *Aedes aegypti* (Diptera: Culicidae), *J. Med. Entomol.*, **27** (1990), 892–898. <https://doi.org/10.1093/jmedent/27.5.892>
44. F. El Moustaid, L. R. Johnson, Modeling temperature effects on population density of the dengue mosquito *Aedes aegypti*, *Insects*, **10** (2019), 393. <https://doi.org/10.3390/insects10110393>
45. H. L. C. Dutra, M. N. Rocha, F. B. S. Dias, S. B. Mansur, E. P. Caragata, L. A. Moreira, Wolbachia blocks currently circulating Zika virus isolates in Brazilian *Aedes aegypti* mosquitoes, *Cell Host Microbe*, **19** (2016), 771–774. <https://doi.org/10.1016/j.chom.2016.04.021>
46. S. Towers, F. Brauer, C. Castillo-Chavez, A. Falconar, A. Mubayi, C. Romero-Vivas, Estimate of the reproduction number of the 2015 Zika virus outbreak in Barranquilla, Colombia, and estimation of the relative role of sexual transmission, *Epidemics*, **17** (2016), 50–55. <https://doi.org/10.1016/j.epidem.2016.10.003>
47. C. Poitras, *Findings Shed New Light on Why Zika Causes Birth Defects in Some Pregnancies*. Available from: <https://ysph.yale.edu/news-article/findings-shed-new-light-on-why-zika-causes-birth-defects-in-some-pregnancies/>.
48. O. Diekmann, J. A. Heesterbeek, M. G. Roberts, The construction of next-generation matrices for compartmental epidemic models, *J. R. Soc. Interface*, **7** (2010), 873–885. <https://doi.org/10.1098/rsif.2009.0386>
49. O. Diekmann, J. A. P. Heesterbeek, *Mathematical Epidemiology of Infectious Diseases: Model Building, Analysis, and Interpretation*, John Wiley & Sons, Ltd., New York, 2000.
50. A. Utarini, C. Indriani, R. A. Ahmad, W. Tantowijoyo, E. Arguni, M. R. Ansari, et al., Efficacy of Wolbachia-infected mosquito deployments for the control of Dengue, *N. Engl. J. Med.*, **384** (2021), 2177–2186. <https://doi.org/10.1056/NEJMoa2030243>
51. S. Marino, I. B. Hogue, C. J. Ray, D. E. Kirschner, A methodology for performing global uncertainty and sensitivity analysis in systems biology, *J. Theor. Biol.*, **254** (2008), 178–196. <https://doi.org/10.1016/j.jtbi.2008.04.011>



AIMS Press

© 2025 the Author(s), licensee AIMS Press. This is an open access article distributed under the terms of the Creative Commons Attribution License (<https://creativecommons.org/licenses/by/4.0>)